Rubisco production in maize mesophyll cells through ectopic expression of subunits and chaperones

Hotto, Amber M; Salesse-Smith, Coralie; Lin, Myat; Busch, Florian A; Simpson, Isabelle; Stern, David B

DOI:
10.1093/jxb/erab189

Document Version
Peer reviewed version

Citation for published version (Harvard):
Hotto, AM, Salesse-Smith, C, Lin, M, Busch, FA, Simpson, I & Stern, DB 2021, 'Rubisco production in maize mesophyll cells through ectopic expression of subunits and chaperones', *Journal of Experimental Botany*, vol. 72, no. 13, 4930–4937, pp. 4930-4937. https://doi.org/10.1093/jxb/erab189

Rubisco production in maize mesophyll cells through ectopic expression of subunits and chaperones

Amber M. Hotto[1,*], Coralie Salesse-Smith[1,2,*], Myat Lin[3], Florian A. Busch[4,5], Isabelle Simpson[1], David B. Stern[1,+]

[1] Boyce Thompson Institute, Ithaca, New York, USA. Amber M. Hotto – amh264@cornell.edu, ORCID ID: 0000-0003-1846-9504; Isabelle Simpson – i2simpson@uwaterloo.ca
[2] Current address: Carl R. Woese Institute for Genomic Biology, University of Illinois, IL 61801, USA. ORCID ID: 0000-0002-2856-4217. ces343@illinois.edu
[3] Cornell University, Ithaca, New York, USA. mtl84@cornell.edu
[4] School of Biosciences, and Birmingham Institute of Forest Research, University of Birmingham, Edgbaston, Birmingham, B15 2TT, United Kingdom. ORCID ID: 0000-0001-6912-0156. F.A.Busch@bham.ac.uk
[5] Research School of Biology, The Australian National University, Canberra, Australian Capital Territory, Australia.

[*] These authors contributed equally to this work

[+] Correspondence: January 29, 2021

Number of Tables: 0
Number of Figures: 5
Word Count: 2,749
Supplementary Figures: 4

Running title: Rubisco production in maize mesophyll cells

Highlight

Rubisco is confined to bundle sheath cells in C_4 plants, increasing the efficiency of CO_2 fixation. Here, we have overcome cell type specificity, adding to the toolkit for engineering photosynthesis.

Abstract

C_4 plants, such as maize, strictly compartmentalize Rubisco to bundle sheath chloroplasts. The molecular basis for the restriction of Rubisco from the more abundant mesophyll chloroplasts is not fully understood. Mesophyll chloroplasts transcribe the Rubisco large subunit gene, and when normally quiescent transcription of the nuclear Rubisco small subunit gene family is overcome by ectopic expression, mesophyll chloroplasts still do not accumulate measurable Rubisco. Here we show that a combination of five ubiquitin promoter-driven nuclear transgenes expressed in maize leads to mesophyll accumulation of assembled Rubisco. These encode the Rubisco large and small subunits, Rubisco Assembly Factors 1 and 2, and the assembly factor Bundle Sheath Defective 2. In these plants Rubisco large subunit accumulates in mesophyll cells, and appears to be assembled into holoenzyme capable of binding the substrate analog CABP. Isotope discrimination assays suggest, however, that mesophyll Rubisco is not participating in carbon assimilation in these plants, most likely due to a lack of the substrate ribulose 1,5-bisphosphate and/or Rubisco activase. Overall, this work defines a minimal set of Rubisco assembly factors *in planta* and may help lead to methods of regulating the C_4 pathway.

Keywords – C_4 photosynthesis, cell type specificity, maize, Rubisco, Rubisco assembly

Abbreviations – BS – bundle sheath cells, M – mesophyll cells

Introduction

Primary carbon assimilation in plants relies on the enzyme Rubisco, which combines CO_2 and ribulose 1,5-bisphosphate (RuBP) to generate two molecules of 3-phosphoglycerate (3-PGA). Rubisco is prone to a wasteful side reaction when O_2 competes with CO_2 at the active site. One evolutionary mechanism that has arisen multiple times to suppress the oxygenation side reaction is the C_4, or Hatch-Slack, pathway (Hatch and Slack, 1966). A common embodiment of the C_4 pathway is initial fixation of CO_2 at its atmospheric concentration by phosphoenolpyruvate carboxylase (PEPC) in mesophyll (M) cells, generating a C_4 intermediate that is shuttled to bundle sheath (BS) cells. CO_2 is released from the intermediate in BS chloroplasts, creating a high CO_2 concentration that diminishes oxygenation.

The C_4 pathway utilizes spatial separation of Rubisco from the initial site of CO_2 fixation. In maize and other species, restriction of Rubisco to BS chloroplasts occurs during leaf development, with leaf maturation coinciding with diminishing Rubisco content in M cells (Patel and Berry, 2008). *A priori*, an absence of M Rubisco could be due to transcriptional, translational and/or post-translational mechanisms. The large and small Rubisco subunits are expressed from chloroplast and nuclear genes, respectively. In maize, run-on transcription showed that the chloroplast *rbcL* gene is active in M chloroplasts from mature tissue, however the resultant transcript accumulates at a relatively low level, suggesting it is unstable (Kubicki *et al.*, 1994). At the same time, *RbcS* promoters appear to be inactive in M cells, as evidenced by yellow fluorescent protein expressed from a transgene driven by the *RbcS* promoter only being visible in BS cells in maize (Sattarzadeh *et al.*, 2010). Activity of the *RbcS* promoter may be regulated by several *cis* elements that both promote BS expression and repress M expression (Viret *et al.*, 1994).

The apparent instability of *rbcL* mRNA and transcriptional silencing of *RbcS* suggested that ensuring high levels of those transcripts might support M expression of Rubisco. Maize plants stably transformed with ubiquitin-promoter-driven *RbcS* and a nuclear-localized *rbcL* gene (LSSS; Fig. 1) did accumulate those transcripts, but not Rubisco holoenzyme in M (Wostrikoff *et al.*, 2012). This suggested that other assembly or stabilizing factors were still lacking in M cells, or that Rubisco is subject to post-translational degradation in this cell type. There are currently three Rubisco-specific and essential assembly factors identified through genetic screens in maize: Bundle Sheath Defective 2 (Bsd2), and Rubisco Accumulation Factors 1 and 2 (Raf1 and Raf2) (Brutnell *et al.*, 1999; Feiz *et al.*, 2012, 2014). Proteomic (Friso *et al.*, 2010) and immunological (Salesse-Smith *et al.*, 2017) data suggest that Bsd2 accumulates both in M and BS, whereas Raf1 and Raf2 are predominantly localized in BS chloroplasts. Whether the Bsd2 level in M chloroplasts would be sufficient to support Rubisco assembly, in addition to its still-undescribed function in this cell type, is unknown.

Here we provide data from plants termed “5X”, where the LSSS transgenes have been stacked with those expressing high levels of Bsd2, Raf1 and Raf2 in both M and BS cells. We show that 5X lines accumulate at least a WT level of Rubisco in BS cells and in addition, Rubisco accumulates in M cells, suggesting that the enzyme is not inherently unstable in this context. M Rubisco in 5X plants does not appear to be active in CO_2 fixation. Nonetheless, the ability to engineer Rubisco accumulation in C_4 M cells could prove useful in helping certain crops become more resilient by switching dynamically between C_4 and C_3 mechanisms.

Materials and Methods

Plant lines and growth conditions

Each maize transgene contains the maize ubiquitin1 promoter and *Nos* terminator assembled with the coding sequence of interest with (LS_N, Raf2, and Bsd2) or without (SS and Raf1) a C-

terminal Flag epitope tag (Fig. 1). Transgene cassettes were introduced into Hi-II maize at the Plant Transformation Core Research Facility at the University of Nebraska–Lincoln via *Agrobacterium*, using the *aadA* streptomycin resistance gene for bacterial selection and the *nptII* kanamycin resistance gene for plant selection. Hi-II is a lab strain of maize that comes from a cross between A188 x B73 and is highly amenable to transformation (Armstrong *et al.*, 1991; Songstad *et al.*, 1996). Details of the LSSS, Raf1 and Bsd2 lines have been previously described (Wostrikoff *et al.*, 2012; Salesse-Smith *et al.*, 2017, 2018); the UBI-Raf2 cassette was introduced using the binary plasmid pPTN1300. Expression of UBI-Raf2 was compared between three independent T1 transgenic events by immunoblot analysis (see *Protein Isolation and Analysis* for details) with the anti-Flag antibody (Fig. S1A). Overexpression of UBI-Raf2 was further confirmed by immunoblot utilizing the anti-Raf2 antibody compared to Hi-II (Fig. S1B, Feiz *et al.*, 2014). The RAF2 antibody cross reacts with non-specific proteins, however, the RAF2 protein can be clearly identified by comparison to a FLAG immunoblot and relative to the Hi-II control. Event 3412 was used as a source for introgressing Raf2 overexpression into other transgenic backgrounds. 5X lines were made by sequentially crossing homozygous Raf1+LSSS to Raf2, and then "4X" progeny to Bsd2. Seed from all lines was germinated in 1/3 metro mix and 2/3 turface calcined clay soil mix and fertilized three times per week. Plants were grown in the greenhouse at 28°C/25°C day/night. Segregating progeny from the cross Raf1-LSSS-Raf2 x Bsd2 were genotyped by immunoblot analysis using anti-Flag and anti-Raf1 antibodies (see protein isolation and analysis below). Hi-II was used as a WT comparator to 5X plants.

Mesophyll protoplast isolation

Mesophyll cells were extracted from ~5 g of leaf tissue taken from the tip of the third and fourth fully-expanded leaves of 2-3 week old plants (~10-15 individuals) largely as described in Markelz *et al.* (2003). Maize leaves contain a developmental gradient from the base (C_3 photosynthesis) to the tip (C_4 photosynthesis), therefore the leaf tip was used for analysis of C_4 photosynthetic tissues because it is fully differentiated. Briefly, tissue was cut transversely into small strips, infiltrated with enzyme buffer (20 mM MES, pH5.5, 1 mM $MgCl_2$, 0.6M sorbitol, 2% Cellulase Onozuka, 0.1% Macerase) under vacuum for ~1.5 min, then digested for 3h at room temperature. Mesophyll protoplasts were released from the tissue with gentle pressure, then filtered through 40 µM nylon mesh. Cells in the filtrate were pelleted by centrifugation at 300xg for 5 min at 4°C, then resuspended in wash buffer (50 mM Tris, pH 7.5, 1 mM $MgCl_2$, 0.6M sorbitol, 100 mM β-mercaptoethanol) and pelleted again. The final pellet was re-suspended in 1 mL of wash buffer, aliquoted into 250 µL samples, concentrated, and the pellets stored at -80°C. For analysis of replicates, batches of 15-20 plants were grown at different times (biological replicates), then ~5 g of leaf tissue was harvested when they were 2-3 weeks old. Each mesophyll replicate, therefore, represents pooled extracts from ~10-15 individual plants of the same line.

Protein isolation and analysis

Total soluble protein was isolated from the tip of the third fully-expanded leaf of ~2-week-old plants on an equal area basis using four hole punches. Samples were immediately placed in liquid nitrogen and ground to a fine powder. Protein homogenization buffer and 2X Laemmli SDS buffer were added to the samples in equal volumes, vortexed, heated at 70°C for 10 min, then centrifuged at high speed for 10 min. The supernatant was loaded into a 13% SDS-polyacrylamide gel, then transferred to polyvinylidene difluoride (PVDF) membranes (Bio-Rad). After blocking for >1h in 5% milk, primary antibodies were incubated with the membrane overnight at 4°C in Tris-buffered saline, 0.1% Tween 20, and 1% milk. Primary antibodies used were anti-LS (1:10000 dilution; Agrisera), anti-Raf1 (1:10000 dilution; Feiz *et al.*, 2012), anti-Raf2 (1:2500 dilution; Feiz *et al.*, 2014), anti-Bsd2 (1:3333; Feiz *et al.*, 2014), anti-PPDK (1:10000 dilution; Agrisera), anti-ME (1:5000 dilution; Agrisera), and anti-Flag (1:5000; Sigma-

Aldrich). Incubation with goat anti-rabbit IR dye 800 CW (LI-COR) secondary antibody was performed at room temperature for 1-2h in the same buffer as the primary antibody, and blots were imaged using the LI-COR Odyssey Infrared Imaging System. Protein bands were quantified using ImageStudio Lite software. For staining, gels were incubated with 0.01% Coomassie Blue R-250 (CBB) and photographed after destaining with 7% acetic acid and 40% methanol. To equalize protein loading from mesophyll preparations, sample volumes were adjusted to yield equal PPDK signal intensity on α-PPDK immunoblots with the assumption that PPDK protein abundance did not vary between lines. Total protein samples extracted from leaf tissue were loaded on an equal leaf area basis.

For native protein separation, 4 µg of total protein or 2.5 µg of mesophyll protein was prepared in 1X NuPAGE native sample buffer with complete protease inhibitor cocktail (Roche) and separated in a 4-16% NuPAGE Bis-Tris gel according to the package instructions. Total soluble native protein determination was completed using the Bio-Rad Protein Assay Dye Reagent according to the manufacturer's protocol using a dilution series of BSA as the standard. Native gels were blotted using the wet transfer Mini Blot Module (ThermoFisher) in 1X NuPAGE non-reducing transfer buffer. Coomassie staining and immunoblot analysis were completed as described above.

Quantification of Rubisco active sites

Radiolabeled carboxyarabinitol bisphosphate (^{14}C-CABP) was synthesized as a ^{14}C-CABP and ^{14}C-CRBP (carboxyribotol bisphosphate) mixture from RuBP (Sigma-Aldrich, 83895) and ^{14}C-KCN (American Radiolabeled Chemicals) as described by Whitney and Sharwood (2014). Each leaf extract was suspended in 0.25-0.30 mL of 20 mM Tris-HCl, pH 9, 250 mM NaCl, 50 mM $NaHCO_3$, 4 mM $MgCl_2$, with Pierce protease inhibitor mini tablets (Thermo Scientific, A32955), and after incubation at 23 °C for 20 min to fully activate all the Rubisco in the samples, 0.1 mL of each supernatant was further incubated with 7.2 nmol of the ^{14}C-CABP + ^{14}C-CRBP mixture at 23°C for 20 min. The ^{14}C-CABP bound to Rubisco was isolated with size-exclusion chromatography using 10 mL of Sephadex G50 fine resin equilibrated with 20 mM bicine NaOH, 75 mM NaCl pH 8.0 in a 0.7 x 30 cm glass column. The resin was washed with 0.2 mL of the same buffer followed by three applications of 0.75 mL of buffer. The eluent was collected for each of the next five applications (0.75 mL, 1.5 mL, 0.75 mL, 0.75 mL and 2.25 mL) of buffer and mixed with 3 mL of Ultima gold liquid scintillation cocktail (PerkinElmer), and the ^{14}C activities were measured with a Beckman LS 6000IC scintillation counter. The Rubisco active sites were calculated as described previously (Whitney and Sharwood, 2014). Total soluble protein was quantified from aliquots of the same samples using the Bio-Rad Protein Assay Dye Reagent, and the concentrations of Rubisco active sites in the extraction buffer in µM were calculated on a total soluble protein basis and presented in Fig. 4.

Isotopic measurements

Leaf samples from Hi-II and 5X plants were individually ground to a fine powder with a ball mill, and 1.5 mg of the resulting powder transferred to individual tin cups. The tin cups were then combusted in an elemental analyzer (Carlo Erba 1110, Milan, Italy) and the resulting CO_2 and N_2 introduced into an isotope ratio mass spectrometer (Micromass Isoprime, Manchester, UK) via a gas chromatograph to quantify %C, %N and $\delta^{13}C$. The $\delta^{13}C$ of the leaf matter was calibrated against known beet ($\delta^{13}C$ = -24.63‰) and cane ($\delta^{13}C$ = -10.45‰) sugar standards measured alongside the leaf samples.

Statistical analysis

The Student's unpaired T-test was used to determine if differences in LS or Rubisco active sites between samples were significant. Specifically, for LS quantified by immunoblot from mesophyll

protein samples, an average of the three replicates was used for the T-test. Each replicate of mesophyll extraction, however, represents 10-15 individual plants of the same line. For total Rubisco active sites per total soluble protein, an average from six (total Hi-II, total 5X or 5X mesophyll) or five (Hi-II mesophyll) samples were used. The total protein samples were taken from six different plants on an equal leaf area basis, while the mesophyll samples represent total soluble protein extracted from tissue pooled from 10-15 plants of a given line.

Results

The five transgenes used in combination to create 5X lines are shown in Figure 1. The LSSS construct contains two UBI-driven transgenes in tandem encoding the two Rubisco structural subunits, with nucleus-encoded LS being denoted LS_N. Each of the other transgenes encodes an assembly factor driven by the UBI promoter, flanked by a Flag epitope tag in the cases of BSD2 and RAF2. Each transgenic line has been previously reported except UBI-RAF2. For this transgene, we performed initial characterization of three independent events and detected transgene expression using anti-Flag (Fig. S1A) or anti-RAF2 (Fig. S1B, left two lanes), which clearly revealed a much higher RAF2 abundance than in the transformation recipient control, Hi-II. RAF2 overexpression did not appear to have any effect on Rubisco or RAF1 accumulation in total leaf protein (Fig. S1A). A single UBI-Raf2 event was used for subsequent crosses.

To create 5X lines, a succession of genetic crosses was performed between transgenic lines. Because of the long generation time of maize, and the need to combine four independently segregating loci (LSSS segregates as a single locus), we did not distinguish between hemizygosity and homozygosity at the transgene loci. Segregants were genotyped from a variety of crosses that were expected to generate 5X progeny in sufficient numbers. This could be accomplished by using anti-Flag to simultaneously detect UBI-LS_N (and by inference UBI-SS), UBI-RAF2 and UBI-BSD2 (Fig. S1B, right panel). UBI-RAF1 was detected using an anti-RAF1 antibody (Feiz *et al.*, 2012). 5X lines were identified many times over a period of years from various segregating seed pools, with no evidence for transgene silencing as deduced from segregation ratios of protein expression, and in addition each locus segregated as would be expected from a single transgene insertion. No gross differences in growth or developmental phenotypes (plant height, leaf morphology and color, maturation time) were observed in the 5X lines compared to the Hi-II control. Detailed measurements of growth characteristics have not yet been completed.

Since our goal was to assess possible Rubisco accumulation and activity in M cells, we harvested leaf tissue from verified 5X plants and prepared M protoplasts. Such preparations inevitably contain traces of BS material. Therefore, we used accumulation of known cell-type specific proteins to assess the purity of different M preparations and used them as benchmarks for the proportion of total leaf protein derived from M cells, as described below.

Figure 2 compares the abundance of transgene and marker proteins between Hi-II and 5X in total protein and from three independent preparations of M cells. In total protein, LS increased slightly in 5X material. Each M preparation also clearly showed increased abundance of LS, as well as the expected increased expression (also in total protein) of RAF1, RAF2 and BSD2. The RAF2 immunoblot (Fig. 2) shows a non-specific upper band consistent between all samples and the RAF2 lower band (marked with an asterisk) that is over-accumulating in the 5X samples compared to Hi-II. The two marker proteins are pyruvate inorganic phosphate dikinase (PPDK), which is considered M-specific, and malic enzyme (ME), which is considered BS-specific. PPDK was used to normalize the total amount of M proteins in each lane, whereas ME was used to reflect the presence of BS cells in the M preparations.

The ratio (in arbitrary units) of (LS–ME):PPDK in M preparations was calculated, which uses contaminating ME as a proxy for BS-derived LS in M preparations. PPDK was used to normalize total protein between samples. The results indicated that in agreement with visual inspection, 5X M cells contained more LS compared to Hi-II (0.74 vs. 0.22, respectively; $P<0.05$; bottom of Fig. 2). Although there are differences between antibody sensitivity, the relative ratio of these numbers clearly show that LS is accumulating in M cells in 5X lines at a significant level that cannot be accounted for by an overall increase in Rubisco on a total leaf protein basis.

The presence of LS is consistent with, but does not prove, the presence of Rubisco holoenzyme. To assess the assembly state of LS in the same M preparations we used native gels, as shown in Figure 3. All preparations showed a single band detected by anti-LS, which migrated at the expected 550 kD position for the holoenzyme. We saw no evidence for monomers or dimers of LS (53 or 106 kD), nor for stalled assembly intermediates (>600 kD) as were observed in the *raf1* and *raf2* mutants using *in vivo* labeling (Feiz *et al.*, 2012, 2014). We cannot assess from these data whether the abundance of any specific assembly factor(s) is limiting holoenzyme accumulation, nor if M Rubisco has a different stability than BS Rubisco.

Another measure of Rubisco assembly is the presence of Rubisco active sites. We used binding of the substrate analog [^{14}C]carboxyarabinitol bisphosphate (CABP) for this purpose, as shown in Figure 4. This assay is useful for quantifying total Rubisco active sites present in each sample but does not reflect the native activation status of the extracted Rubisco. Additionally, the M samples represent a fraction of an extract taken from 10-15 plants, therefore this data cannot be presented on a leaf area basis. Therefore, the Rubisco active sites were normalized to total protein quantified from each sample using the Bradford assay. In mesophyll preparations, an approximate doubling of binding sites was measured in 5X compared to Hi-II ($P<0.05$), consistent with immunoblot data. We assume that the binding sites detected in Hi-II M cells, and a roughly equivalent number in 5X, are due to presence of BS material in the M cell preparations.

The presence of assembled Rubisco in M cells raised the intriguing question of whether the enzyme might be catalyzing CO_2 fixation similar to C_3 plants. While CO_2 is present in M cells, the occurrence of RuBP and Rubisco activase (or Rubisco inhibitors) is ambiguous. RuBP is assumed to be BS-specific; it is used as a marker for that cell type, and Rubisco activase is similarly understood to be a BS-specific enzyme, which is supported (but not in an absolute sense) by quantitative proteomic data (Friso *et al.*, 2010). To investigate whether M Rubisco might contribute to carbon assimilation in 5X plants, we used isotopic labeling. Initial fixation of CO_2 in C_4 plants is a process that involves CO_2 dissolution, hydration and PEPC activity, which results in a net discrimination against ^{12}C, whereas in C_3 plants CO_2 is fixed by Rubisco, which discriminates against ^{13}C (Farquhar, 1983). If Rubisco in M cells is functional, then the $\delta\ ^{13}$C ratio would shift toward that of a C_3 plant ($\delta^{13}C$ = -29 to -25‰ for C_3 plants versus $\delta^{13}C$ = -13.5 to -11.5‰ for C_4). Results shown in Figure 5 do not support a change in the $\delta^{13}C$ ratio between Hi-II and 5X plants, suggesting that no significant contribution to CO_2 assimilation is being made by Rubisco in M cells. Measurements made concomitantly showed, however, small decreases and increases, respectively, in %C and %N (Fig. S2). The basis for this modest variation was not further explored. In keeping with these observations, leaf CO_2 assimilation rates under saturating light conditions and varying CO_2 concentrations between Hi-II and 5X plants were not appreciably different (Fig. S3).

Discussion

Here we have shown that Rubisco holoenzyme can be assembled in maize M cells, presumably in chloroplasts, by co-expression of five transgenes under control of the maize ubiquitin

promoter. Using this promoter served several purposes. In the case of LS, the native chloroplast *rbcL* gene is transcribed in M chloroplasts but the transcript is unstable. We therefore introduced an ectopic gene outside the chloroplast, having shown that nucleus-encoded LS is compatible with Rubisco assembly in BS chloroplasts (Wostrikoff *et al.*, 2012). The SS gene is silenced in M cells in a light-dependent manner (see Introduction). Our data suggest that the UBI promoter is effective at engendering M expression, at least to the level required for some assembly of Rubisco.

RAF1, RAF2 and BSD2 were also overexpressed in the 5X line. In wild-type plants, RAF1 and RAF2 are largely confined to BS chloroplasts, and their absence from M chloroplasts is likely to be the reason why Rubisco did not assemble in LSSS transgenics. BSD2, however, accumulates in M and BS cells of wild-type plants. The function of M cell-localized BSD2 may be related to chloroplast morphology (Li *et al.*, 2020), however genetic removal of M expression did not overtly affect maize growth or development, contrary to BSD2 removal from BS cells (Salesse-Smith *et al.*, 2017). In 5X plants, BSD2 expression in both BS and M cells is greatly augmented (Fig. 2), perhaps boosting the potential for Rubisco accumulation in M cells. Preliminary comparisons between 4X plants (without either UBI-BSD2, or UBI-RAF2) and 5X plants support this contention (Fig. S4).

Our results suggest that M cells of 5X plants possess all essential components for assembly and stabilization of Rubisco. This mirrors *in vitro* findings that besides chloroplast GroEL/GroES homologs, RAF1, RAF2 and BSD2 are the only factors required to assemble Arabidopsis Rubisco in bacterial cells (Aigner *et al.*, 2017). Another auxiliary factor, RBCX, enhanced *in vitro* assembly by approximately 2-fold but was not required. RBCX is expressed in maize, however its cell type distribution has not been fully evaluated (Li *et al.*, 2010; Wang *et al.*, 2018). It is possible that enhancing its expression in M cells would augment current results with 5X plants. Similarly, the GroEL homolog CPN60α1/CPS2 appears to be particularly important for Rubisco assembly *in planta* (Barkan, 1993; Kim *et al.*, 2013). Proteomics suggest that CPS2 is not cell type-specific, however its level of M expression could limit the ability of 5X plants to accumulate M Rubisco.

Our data indicate that Rubisco in 5X M cells is not contributing to carbon assimilation, likely due to a lack of RuBP substrate, a failure to activate the enzyme, and/or missing acetylation, phosphorylation or other post-translational modifications (Grabsztunowicz *et al.*, 2017), which could in turn limit holoenzyme stability. The ability to activate M-localized Rubisco would impart C_3-like character to those plants, in terms of initial carbon assimilation. Given that C_4 plants only have growth advantages under a narrow range of environmental conditions, the ability to switch plants between C_4 and C_3 pathways could be beneficial. This switch occurs naturally in some species during development, for example in maize along the leaf gradient, and between aerial and submerged tissues or within single cells in certain aquatic plants (Ueno *et al.*, 1988; Bowes, 2011; Koteyeva *et al.*, 2016). There are also a number of species, however, that switch dynamically between the C_3 and Crassulacean acid metabolism pathways, for example in response to drought or salinity stress (Winter *et al.*, 2008; reviewed in Heyduk *et al.*, 2019). A dynamic switch between C_3 and C_4 photosynthesis may be viewed as evolutionary intermediates towards a pure C_4 state, but also as an advantageous photosynthetic plasticity that could potentially benefit crop plants subjected to repeated abiotic stress.

Supplementary Data

Figure S1. Genotyping transgenic lines by immunoblot analysis.

Figure S2. Isotope and GC-MS analysis of percent C and percent N.

Figure S3. CO_2 response (A-Ci) curves for Hi-II and 5X plants are not significantly different.

Figure S4. Immunoblot analysis of mesophyll cell protein extracted from transgenic maize lines compared to Hi-II (WT).

Acknowledgements

We would like to thank Tom Clemente and Shirley Sato (University of Nebraska-Lincoln) for assembling the final Raf2 transformation construct, performing maize transformation, and providing seed from T0 lines. We also thank H. Stuart-Williams (Australian National University) for technical help with the isotope analysis. This work was supported by the Agriculture and Food Research Initiative (awards 2016-67013-24464 and #2020-67013-30911, Stern Laboratory) from the USDA National Institute of Food and Agriculture, and the Department of Energy Biosciences award DE-SC-0020142 (Hanson Laboratory).

Author Contributions

AMH contributed to experimental oversight and execution for Figures 1-4 and S1, and manuscript writing. CS participated in experimental design, including creating the constructs, and experimental oversight for Figure S3. ML executed experiments for Figure 4, and FAB executed experiments for Figure 5 and S2. IS contributed to Figures 2 and 3. DBS participated in experimental design, data analysis, project oversight and manuscript writing. AMH, CS, ML, FAB and DBS contributed to manuscript editing.

Data Availability

All data supporting the findings described here are present in the article and in the supplementary data. Novel transgenic maize lines described in the paper are available for non-commercial research use and can be obtained by contacting the corresponding author.

References

Aigner H, Wilson RH, Bracher A, Calisse L, Bhat JY, Hartl FU, Hayer-Hartl M. 2017. Plant RuBisCo assembly in E. coli with five chloroplast chaperones including BSD2. Science (New York, N.Y.) **358**, 1272–1278.

Armstrong CL, Green CE, Philips RL. 1991. Development and availability of germplasm with high type II culture formation response. Maize Genetics Cooperation Newsletter, 92–93.

Barkan A. 1993. Nuclear mutants of maize with defects in chloroplast polysome assembly have altered chloroplast RNA metabolism. Plant Cell **5**, 389–402.

Bowes G. 2011. Chapter 5 Single-Cell C4 Photosynthesis in Aquatic Plants. In: Raghavendra AS,, In: Sage RF, eds. C4 Photosynthesis and Related CO2 Concentrating Mechanisms. Dordrecht: Springer Netherlands, 63–80.

Brutnell TP, Sawers RJ, Mant A, Langdale JA. 1999. BUNDLE SHEATH DEFECTIVE2, a novel protein required for post- translational regulation of the rbcL gene of maize. Plant Cell **11**, 849–864.

Farquhar GD. 1983. On the nature of carbon isotope discrimination in C4 species. Functional Plant Biology **10**, 205–226.

Feiz L, Williams-Carrier R, Belcher S, Montano M, Barkan A, Stern DB. 2014. A protein with an inactive pterin-4a-carbinolamine dehydratase domain is required for Rubisco biogenesis in plants. Plant Journal **80**, 862–869.

Feiz L, Williams-Carrier R, Wostrikoff K, Belcher S, Barkan A, Stern DB. 2012. Ribulose-1,5-Bis-Phosphate Carboxylase/Oxygenase Accumulation Factor1 is required for holoenzyme assembly in maize. Plant Cell **24**, 3435–3446.

Friso G, Majeran W, Huang M, Sun Q, van Wijk KJ. 2010. Reconstruction of metabolic pathways, protein expression and homeostasis machineries across maize bundle sheath and mesophyll chloroplasts; large scale quantitative proteomics using the first maize genome assembly. Plant Physiology **152**, 1219–1250.

Grabsztunowicz M, Koskela MM, Mulo P. 2017. Post-translational modifications in regulation of chloroplast function: Recent advances. Frontiers in Plant Science **8**, 240.

Hatch MD, Slack CR. 1966. Photosynthesis by sugar-cane leaves. A new carboxylation reaction and the pathway of sugar formation. The Biochemical journal **101**, 103–111.

Heyduk K, Moreno-Villena JJ, Gilman IS, Christin PA, Edwards EJ. 2019. The genetics of convergent evolution: insights from plant photosynthesis. Nature Reviews Genetics **20**, 485–493.

Kim SR, Yang JI, An G. 2013. OsCpn60α, encoding the plastid chaperonin 60α subunit, is essential for folding of rbcL. Mol. Cells **35**, 402–409.

Koteyeva NK, Voznesenskaya E V, J OB, Cousins AB, Edwards GE. 2016. The unique structural and biochemical development of single cell C4 photosynthesis along longitudinal leaf gradients in Bienertia sinuspersici and Suaeda aralocaspica (Chenopodiaceae). Journal of Experimental Botany.

Kubicki A, Steinmuller K, Westhoff P. 1994. Differential transcription of plastome-encoded genes in the mesophyll and bundle-sheath chloroplasts of the monocotyledonous NADP-malic enzyme-type C4 plants maize and Sorghum. Plant Molecular Biology **25**, 669–679.

Li H, Bai M, Jiang X, Shen R, Wang H, Wang H, Wu H. 2020. Cytological evidence of BSD2 functioning in both chloroplast division and dimorphic chloroplast formation in maize leaves. BMC Plant Biology **20**, 1–8.

Li P, Ponnala L, Gandotra N, *et al.* 2010. The developmental dynamics of the maize leaf transcriptome. Nature Genetics **42**, 1060–1067.

Markelz NH, Costich DE, Brutnell TP. 2003. Photomorphogenic responses in maize seedling development. Plant Physiology **133**, 1578–1591.

Patel M, Berry JO. 2008. Rubisco gene expression in C4 plants. Journal of Experimental Botany **59**, 1625–1634.

Salesse-Smith CE, Sharwood RE, Busch FA, Kromdijk J, Bardal V, Stern DB. 2018. Overexpression of Rubisco subunits with RAF1 increases Rubisco content in maize. Nature Plants **4**, 802–810.

Salesse-Smith C, Sharwood RE, Sakamoto W, Stern DB. 2017. The Rubisco chaperone BSD2 may regulate chloroplast coverage in maize bundle sheath cells. Plant Physiology **175**, 1624–1633.

Sattarzadeh A, Fuller J, Moguel S, Wostrikoff K, Sato S, Covshoff S, Clemente T, Hanson M, Stern DB. 2010. Transgenic maize lines with cell-type specific expression of fluorescent proteins in plastids. Plant Biotechnology Journal **8**, 112–125.

Songstad DD, Armstrong CL, Petersen WL, Hairston B, Hinchee MAW. 1996. Production of transgenic maize plants and progeny by bombardment of hi-II immature embryos. In Vitro Cellular & Developmental Biology - Plant **32**, 179–183.

Ueno O, Samejima M, Muto S, Miyachi S. 1988. Photosynthetic characteristics of an amphibious plant, Eleocharis vivipara: Expression of C4 and C3 modes in contrasting environments. Proceedings of the National Academy of Sciences **85**, 6733–6737.

Viret JF, Mabrouk Y, Bogorad L. 1994. Transcriptional photoregulation of cell-type-preferred expression of maize RBCS-m3: 3’ and 5’ sequences are involved. Proceedings of the National Academy of Sciences USA **91**, 8577–8581.

Wang B, Li Z, Ran Q, Li P, Peng Z, Zhang J. 2018. ZmNF-YB16 overexpression improves drought resistance and yield by enhancing photosynthesis and the antioxidant capacity of maize plants. Frontiers in Plant Science **9**, 1–14.

Whitney SM, Sharwood RE. 2014. Plastid transformation for rubisco engineering and protocols for assessing expression. Methods in Molecular Biology **1132**, 245–262.

Winter K, Garcia M, Holtum JAM. 2008. On the nature of facultative and constitutive CAM: environmental and developmental control of CAM expression during early growth of Clusia, Kalanchoë, and Opuntia. Journal of Experimental Botany **59**, 1829–1840.

Wostrikoff K, Clark A, Sato S, Clemente T, Stern D. 2012. Ectopic expression of rubisco subunits in maize mesophyll cells does not overcome barriers to cell type-specific accumulation. Plant Physiology **160**, 419–432.

Figure Legends

Figure 1. Transgenes used in this study.

P_{UBI}, maize ubiquitin promoter; RbcS, maize Rubisco small subunit, $RbcL_N$, nuclear codon-optimized version of the maize chloroplast Rubisco large subunit gene with Flag epitope tag and the RbcS chloroplast transit peptide (TP); Raf1 and Raf2, maize Rubisco Accumulation Factor1 and 2, respectively; Bsd2, maize Bundle Sheath Defective 2. The native transit peptide was retained for *RbcS, Raf1, Raf2,* and *Bsd2* transgenes*.* All transgenes utilize the Nos terminator (Nos_T).

Figure 2. Increased LS accumulation in mesophyll cells of 5X plants.

Total soluble leaf protein (left two lanes, loaded on an equal leaf area basis), or soluble protein extracted from mesophyll protoplasts (remaining lanes, loaded to yield equal PPDK intensity) was analyzed for the proteins indicated at left by immunoblot. Protein sizes are indicated at the right (kDa). Rep 1, 2, 3, refer to independent extractions of M proteins from pooled leaf tissue (10-15 plants each) from separately grown plants. Relative levels of LS in M preparations were estimated by quantifying the ratio of LS minus ME to PPDK signal intensity in the three replicates, using a Student's unpaired t-test ($P<0.0365$, $n=3$). Bands corresponding to Raf2 and ME are marked with a white asterisk. Hi-II: control; 5X: maize line containing the 5 transgenes detailed in Fig. 1; CBB: Coomassie stain.

Figure 3. Mesophyll-localized LS is assembled into Rubisco in 5X plants.

Total soluble leaf protein (left two lanes, loaded on an equal leaf area basis), or soluble protein extracted from mesophyll protoplasts (remaining lanes, loaded based on total soluble protein determined by Bradford assay) was separated in a native gel and analyzed for RbcL by immunoblot. Rep 1, 2, 3, refer to pooled leaf tissue from independent extractions of M proteins from separately grown plants (10-15 plants per extraction). Hi-II: control; 5X: maize line containing the 5 transgenes detailed in Fig. 1; CBB: Coomassie stain.

Figure 4. Average Rubisco active sites (μM) normalized to total soluble protein.

Rubisco active sites were measured using the ^{14}C-CABP method and normalized to total soluble leaf protein, or total soluble protein isolated from M protoplasts, quantified using a Bradford assay. Definitions of Hi-II and 5X are as in Fig. 2. *p=0.015 calculated from a Student's unpaired, two-tailed T-test. n=6, except for Hi-II mesophyll n=5. Total: total soluble leaf protein where each replicate (n) represents a different plant; Mesophyll: mesophyll extractions from pooled leaf samples where each replicate (n) is an independent extraction.

Figure 5. Leaf carbon isotope ratio (δ13C ‰) in Hi-II and 5X plants.

Error bars represent the standard deviation; n=12. Results were benchmarked to C_3 plants using samples from sunflower (Fig. S2). Definitions of Hi-II and 5X are as in Fig. 2.

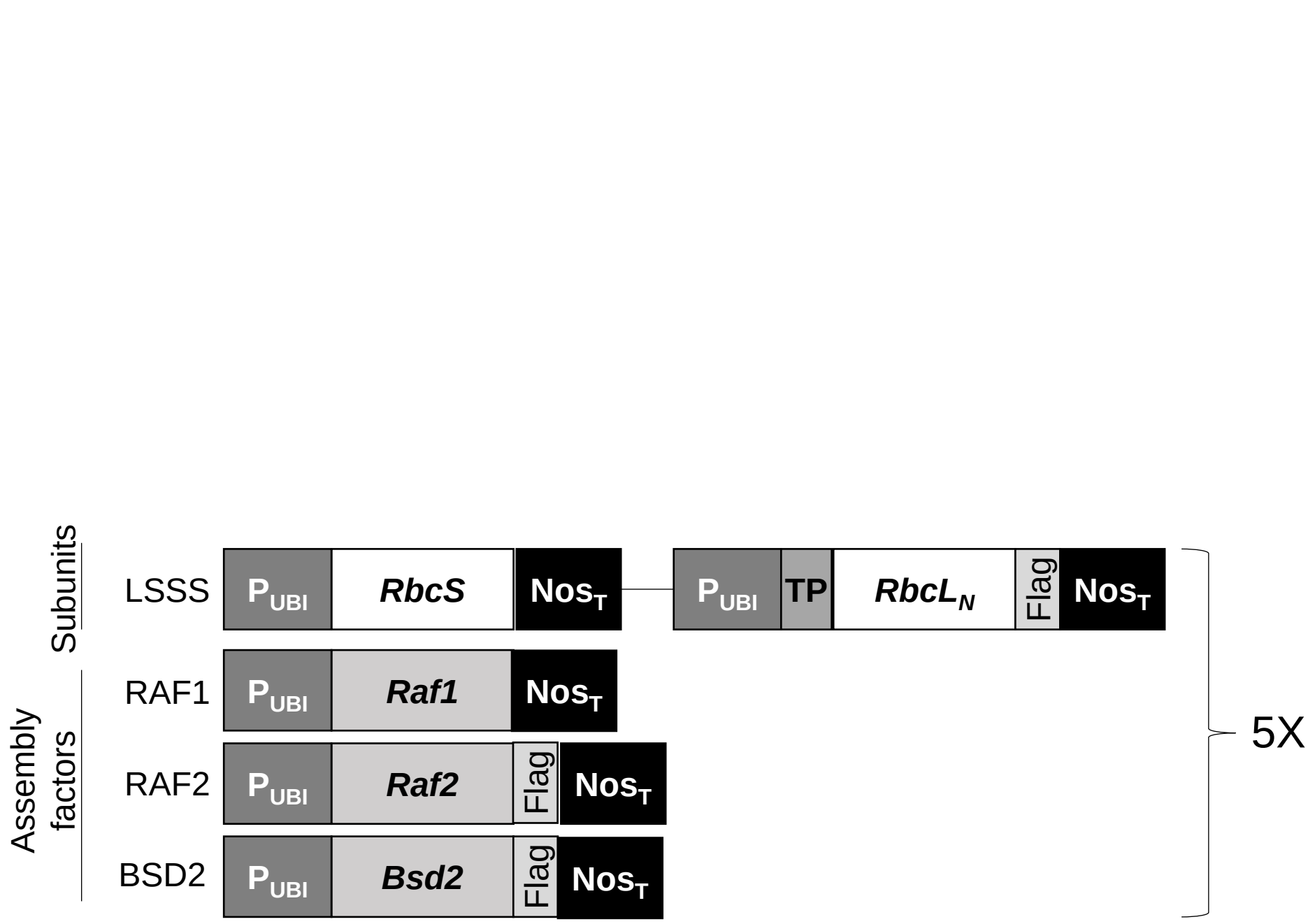

Figure 1. Transgenes used in this study.
P_{UBI}, maize ubiquitin promoter; RbcS, maize Rubisco small subunit, $RbcL_N$, nuclear codon-optimized version of the maize chloroplast Rubisco large subunit gene with Flag epitope tag and the RbcS chloroplast transit peptide (TP); Raf1 and Raf2, maize Rubisco Accumulation Factor1 and 2, respectively; Bsd2, maize Bundle Sheath Defective 2. The native transit peptide was retained in the RbcS, Raf1, Raf2, and Bsd2 transgenes. All transgenes utilize the Nos terminator (Nos_T).

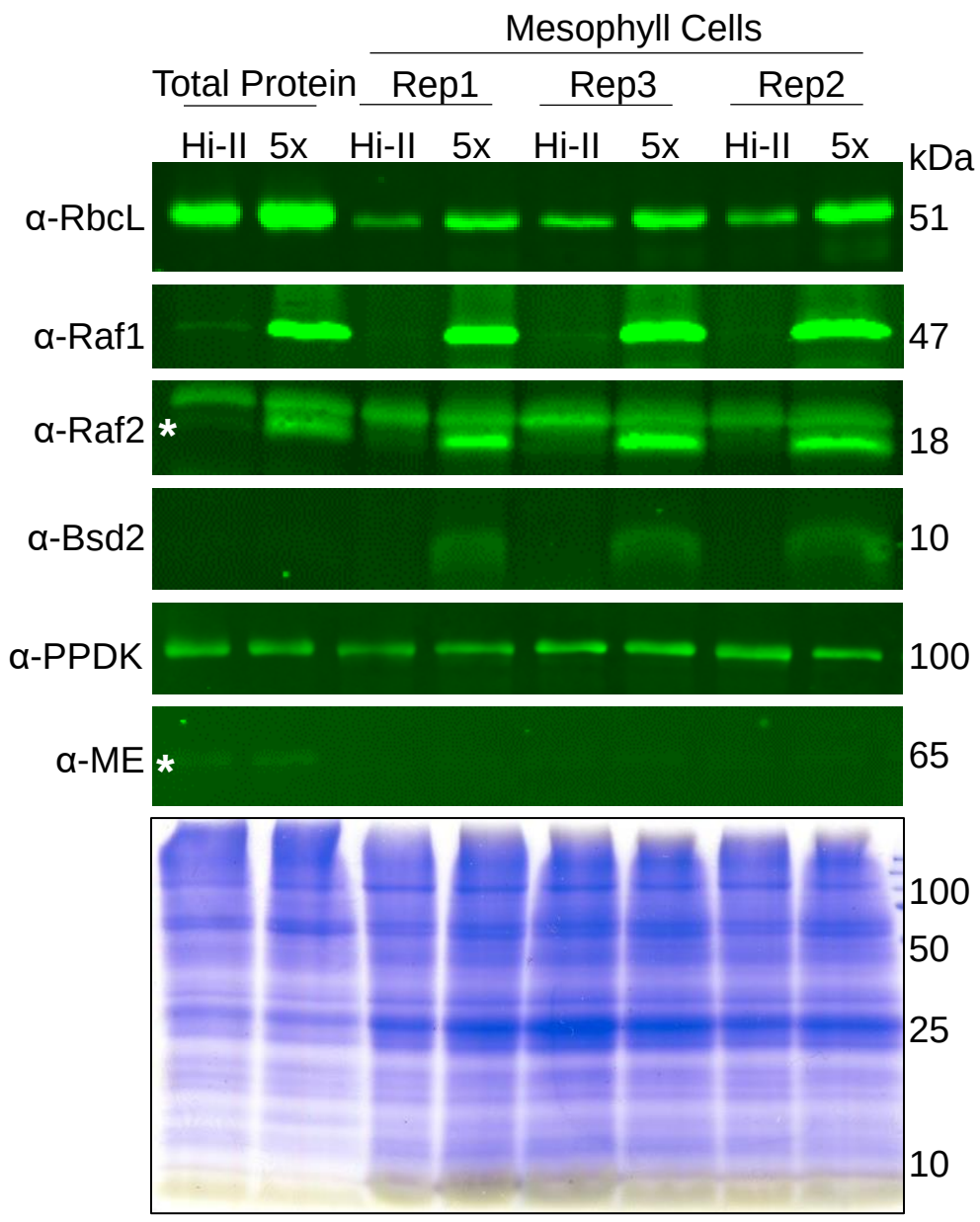

(LS-ME):PPDK in mesophyll
WT: 0.220 ± 0.036
5X: 0.737±0.287
P= 0.036

Figure 2. **Increased LS accumulation in mesophyll cells of 5X plants.** Total soluble leaf protein from individual plants (left two lanes, loaded on an equal leaf area basis), or soluble protein extracted from mesophyll protoplasts (remaining lanes, loaded to yield equal PPDK intensity) was analyzed for the proteins indicated at left by immunoblot. Protein sizes are indicated at the right (kDa). Rep 1, 2, 3, refer to independent extractions of M proteins from pooled leaf tissue (10-15 plants each) from separately grown plants. Relative levels of LS in M preparations were estimated by quantifying the ratio of LS minus ME to PPDK signal intensity in the three replicates. Statistical differences were estimated using a Student's unpaired t-test ($P<0.0365$, $n=3$). Bands corresponding to Raf2 and ME are marked with a white asterisk. Hi-II: control; 5X: maize line containing the 5 transgenes detailed in Fig. 1; CBB: Coomassie stain.

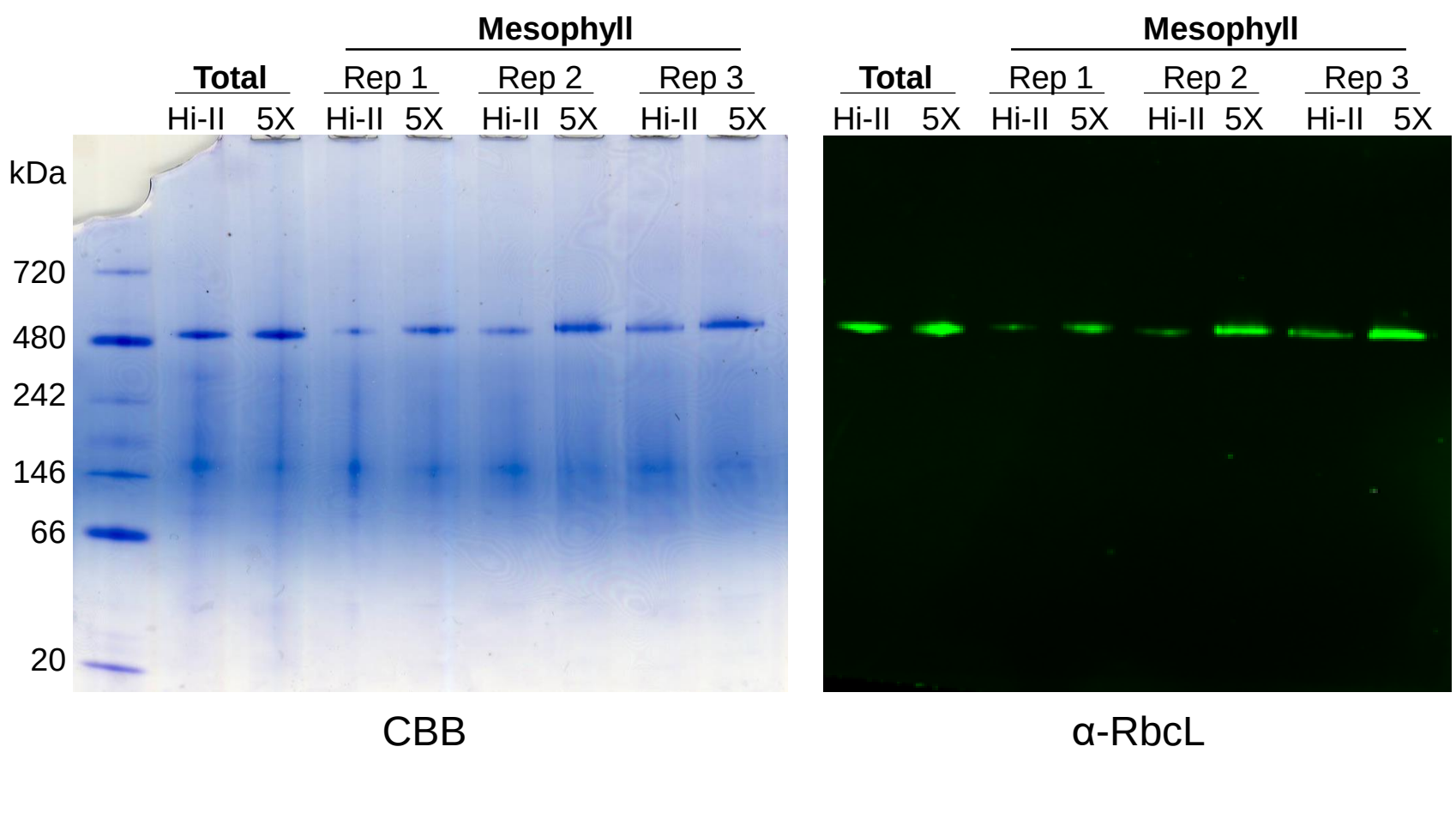

Figure 3. **Mesophyll-localized LS is assembled into Rubisco in 5X plants.**

Total soluble leaf protein (left two lanes, loaded on an equal leaf area basis), or soluble protein extracted from mesophyll protoplasts (remaining lanes, loaded based on total soluble protein determined by Bradford assay) was separated in a native gel and analyzed for RbcL by immunoblot. Rep 1, 2, 3, refer to pooled leaf tissue from independent extractions of M proteins from separately grown plants (10-15 plants per extraction). Hi-II: control; 5X: maize line containing the 5 transgenes detailed in Fig. 1; CBB, Coomassie stain.

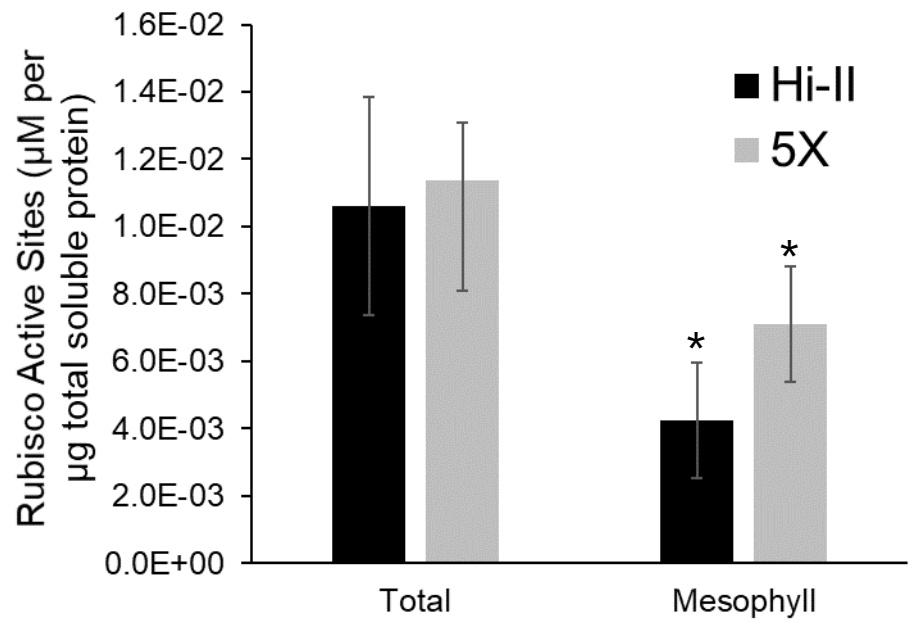

Figure 4. Average Rubisco active sites (µM) normalized to total soluble protein.

Rubisco active sites were measured using the ^{14}C-CABP method and normalized to total soluble leaf protein, or total soluble protein isolated from M protoplasts, quantified using a Bradford assay. Definitions of Hi-II and 5X are as in Fig. 2. *P=0.022 calculated from a Student's unpaired, two-tailed T-test. n=6, except for Hi-II mesophyll n=5. Error bars represent standard deviation. Total: total soluble leaf protein where each replicate (n) represents a different plant; Mesophyll: mesophyll extractions from pooled leaf samples where each replicate (n) is an independent extraction.

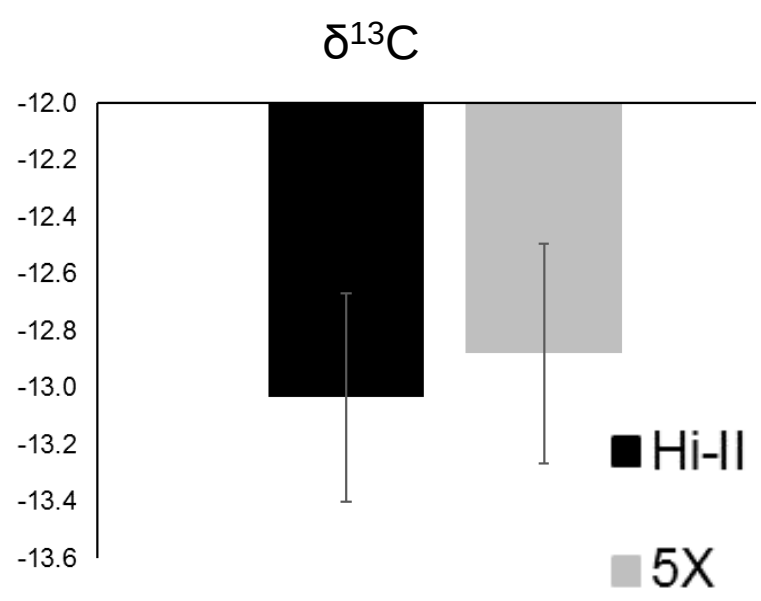

Figure 5. Leaf carbon isotope ratio (δ13C ‰) in Hi-II and 5X plants.
Error bars represent the standard deviation; n=12. Results were benchmarked to C_3 plants using samples from sunflower (Fig. S2). Definitions of Hi-II and 5X are as in Fig. 2.